arXiv:1611.05576v1 [math.NA] 17 Nov 2016

MULTIGRID METHODS FOR A MIXED FINITE ELEMENT METHOD OF THE DARCY-FORCHHEIMER MODEL

JIAN HUANG, LONG CHEN, HONGXING RUI

Abstract. An efficient multigrid method for a mixed finite element method of the Darcy-Forchheimer model is constructed in this paper. A Peaceman-Rachford type iteration is used as a smoother to decouple the nonlinearity from the divergence constraint. The nonlinear equation can be solved element wise with a closed formulae. The linear saddle point system for the constraint is further reduced into a symmetric positive definite system of Poisson type. Furthermore an empirical choice of the parameter used in the splitting is found. By comparing the number of iterations and CPU time of different solvers in several numerical experiments, our method is shown to convergent with a rate independent of the mesh size and the nonlinearity parameter and the computational cost is nearly linear.

1. Introduction

Darcy's law

$$\boldsymbol{u} = -\frac{\boldsymbol{K}}{\mu}\nabla p,$$

describes the linear relationship between the velocity of the creep flow and the gradient of the pressure, which is valid when the Darcy velocity is extremely small [2]. Forchheimer in [8] carried out flow experiments and pointed out that when the velocity of the flow is relatively high, Darcy's law should be replaced by the so-called Darcy-Forchheimer (DF) equation by adding a quadratic nonlinear term to the velocity, shown as follows:

$$\frac{\mu}{\rho}\boldsymbol{K}^{-1}\boldsymbol{u} + \frac{\beta}{\rho}|\boldsymbol{u}|\,\boldsymbol{u} + \nabla p = \boldsymbol{0}.$$

A theoretical derivation of the Darcy-Forchheimer equation can be found in [17].

In recent years, many numerical methods of the Darcy-Forchheimer equation have been developed. A mixed finite element method with a semi-discrete scheme for the time dependent problem was considered by Park in [12]. Pan and Rui in [11] gave a mixed element method for the Darcy-Forchheimer problem based on the Raviart-Thomas (RT) element or the Brezzi-Douglas-Marini (BDM) element. Rui and Pan in [15] proposed the block-centered finite difference method for the Darcy-Forchheimer model, which was thought of as the lowest-order Raviart-Thomas mixed element with proper quadrature formula. Rui, Zhao and Pan in [16] presented a block-centered finite difference method for Darcy-Forchheimer model with variable Forchheimer number. Wang and Rui in [19] constructed a stabilized Crouzeix-Raviart (CR) element for the Darcy-Forchheimer

The work of the authors Jian Huang and Hongxing Rui was supported by the National Natural Science Foundation of China Grant No. 91330106, 11171190. Long Chen was supported by NSF Grant DMS-1418934 and in part by NIH Grant P50GM76516. The work of the author Jian Huang was supported by 2014 China Scholarship Council (CSC).

equation. Rui and Liu in [14] introduced a two-grid block-centered finite difference method for the Darcy-Forchheimer model.

Girault and Wheeler in [9] proved the existence and uniqueness of the solution of the Darcy-Forchheimer model. They approximated the velocity and the pressure by piecewise constant and nonconforming CR elements, respectively. They also suggested an alternating directions iterative method to solve the nonlinear system. The convergences of both the iterative algorithm and the mixed finite element scheme are also proved. López, Molina and Salas in [10] carried out numerical tests of the methods studied in [9], and compared with the Newton's method for solving this problem.

Since it is a nonlinear system, an iterative method should be used, which could be very computationally expensive if the convergence of nonlinear iteration is slow. Multigrid method is one of the most efficient methods on solving the nonlinear elliptic systems. It should be clarified that we no longer have a simple linear residual equation, which is the most significant difference between linear and nonlinear systems. The multigrid scheme we used here is the most commonly used nonlinear version of multigrid. It is called the *full approximation scheme* (FAS) [3] because the problem in the coarse grid is solved for the full approximation rather than the correction; see Section 5 for details.

We use piecewise constant and piecewise linear polynomial to discretize the velocity and the pressure, respectively. We shall apply FAS to construct an efficient V-cycle multigrid method for the nonlinear Darcy-Forchheimer equation and demonstrate the efficiency of our multigrid method. We use the Peaceman-Rachford (PR) type iteration developed in [9] as a smoother. The most relevant work is [10] and our improvement are: 1. We choose a smaller value of the stopping criterion by achieving a better approximation of the pressure accuracy. 2. We report a better choice of the parameter α for decoupling the nonliearity from the constraint rather than the suggested value $\alpha = 1$ for different values of β, and show the advantage of our choice by comparing the number of iterations and CPU time. 3. We carry out some experiments to show the efficiency of our multigrid solver by comparing with the PR iterative solvers. 4. We reduce the saddle point system into a Poisson system and demonstrate the efficiency of our approach.

The remainder of this article is organized as follows: The model problem is demonstrated in Section 2. The mixed weak formulation and the discrete weak formulation are presented in Section 3. The PR iteration and an efficient solver for the linear saddle point systems are posted in Section 4. We construct a V-cycle multigrid scheme by applying FAS for the nonlinear problem in Section 5. Some numerical experiments using our multigrid method are carried out in Section 6 to verify that the efficiency of our method in comparison with solving this nonliear problem using the other iterative methods. Finally, conclusions, and further ideas are presented in Section 7.

2. The Problem and Notation

We consider the steady Darcy-Forchheimer flow of a single phase fluid in a porous medium in a two-dimensional bounded domain Ω, with Lipschitz continuous boundary $\partial\Omega$:

$$\frac{\mu}{\rho}\boldsymbol{K}^{-1}\boldsymbol{u} + \frac{\beta}{\rho}|\boldsymbol{u}|\,\boldsymbol{u} + \nabla p = \boldsymbol{f} \text{ in } \Omega, \tag{2.1}$$

with the divergence constraint

$$\operatorname{div}\boldsymbol{u} = g \text{ in } \Omega, \tag{2.2}$$

and Neumann boundary conditions,

$$\boldsymbol{u}\cdot\boldsymbol{n}=g_N \text{ on } \partial\Omega, \tag{2.3}$$

where $\boldsymbol{u}$ and p are the velocity vector and the pressure, respectively; μ, ρ and β are given positive constants that represent the viscosity of the fluid, its density and its dynamic viscosity, respectively; $|\cdot|$ denotes the Euclidean vector norm $|\boldsymbol{u}|^2=\boldsymbol{u}\cdot\boldsymbol{u}$, $\boldsymbol{n}$ is the unit exterior normal vector to the boundary of the given domain Ω; $\boldsymbol{K}$ is the permeability tensor, assumed to be uniformly positive definite and bounded. According to the divergence theorem, g and g_N are given given functions satisfying the compatibility condition

$$\int_\Omega g\,(x)dx=\int_{\partial\Omega} g_N\,(\sigma)d\sigma. \tag{2.4}$$

We use the standard notations of the Sobolev spaces and the associated norms, see e.g.[1]. We also use the space

$$L_0^2\,(\Omega)=\left\{v\in L^2\,(\Omega):\int_\Omega v\,(\boldsymbol{x})\,d\boldsymbol{x}=0\right\}.$$

3. Weak Formulation

In this section, we define the function spaces as follows:

$$\begin{aligned} X &= L^3(\Omega)^2,\\ M &= W^{1,\frac{3}{2}}(\Omega)\cap L_0^2\,(\Omega)\,. \end{aligned}$$

where the zero mean value condition is added because p is only defined by the (2.1)-(2.3) up to an additive constant. Given $f\in L^3(\Omega), g\in L^{\frac{3}{2}}\,(\partial\Omega)$, the variational formulation is: find a pair $(\boldsymbol{u},p)$ in $X\times M$ such that

$$\begin{aligned} &\frac{\mu}{\rho}\int_\Omega\left(\boldsymbol{K}^{-1}\boldsymbol{u}\right)\cdot\boldsymbol{\varphi}\,d\boldsymbol{x}+\frac{\beta}{\rho}\int_\Omega|\boldsymbol{u}|\,(\boldsymbol{u}\cdot\boldsymbol{\varphi})\,d\boldsymbol{x}\\ &\qquad+\int_\Omega\nabla p\cdot\boldsymbol{\varphi}\,d\boldsymbol{x}=\int_\Omega\boldsymbol{f}\cdot\boldsymbol{\varphi}\,d\boldsymbol{x},\quad\forall\boldsymbol{\varphi}\in X, \end{aligned} \tag{3.1}$$

$$\int_\Omega\nabla q\cdot\boldsymbol{u}\,d\boldsymbol{x}=-\int_\Omega gq\,d\boldsymbol{x}+\int_{\partial\Omega}g_Nq\,d\boldsymbol{x},\quad\forall q\in M. \tag{3.2}$$

The variational formulation (3.1), (3.2) and the original problem (2.1)-(2.3) are equivalent by using the Green's formula:

$$\int_\Omega\boldsymbol{v}\cdot\nabla q\,dx=-\int_\Omega q\,\mathrm{div}\,\boldsymbol{v}\,dx+\langle q,\boldsymbol{v}\cdot\boldsymbol{n}\rangle_{\partial\Omega},\quad\forall q\in M,\forall\boldsymbol{v}\in H, \tag{3.3}$$

where

$$H=\left\{\boldsymbol{v}\in L^3(\Omega)^2:\mathrm{div}\,\boldsymbol{v}\in L^{\frac{6}{5}}\,(\Omega)\right\}.$$

If the given functions g and g_N satisfy the compatibility condition (2.4), then the problem has a unique solution $(\boldsymbol{u},p)$ in $X\times M$ [9].

Let Ω be a polygon in two dimensions which can be completely triangulated by triangles. Let $\mathcal{T}_1$ be a triangulation of Ω, and the triangulations $\mathcal{T}_k\,(k=2,3,\ldots)$ be obtained form $\mathcal{T}_1$ via regular

subdivision, i.e. edge midpoints in $\mathcal{T}_{k-1}$ are connected by new edges to form $\mathcal{T}_k$. Therefore, $\mathcal{T}_k$ is a family of conforming triangulations of $\overline{\Omega}$,

$$\overline{\Omega} = \bigcup_{T\in\mathcal{T}_k} T \quad \text{for } k = 1, 2, 3, \dots,$$

The family $\mathcal{T}_k$ is regular (also called non-degenerate) in the sense of Ciarlet [6].

We discretize $\boldsymbol{u}$ and p in different finite element spaces. The velocity $\boldsymbol{u}$ is approximated in the following space:

$$X_k = \left\{ \boldsymbol{v} \in L^2(\Omega)^2 : \forall T \in \mathcal{T}_k, \boldsymbol{v}|_T \in \mathbb{P}_0^2 \right\}, \tag{3.4}$$

and the pressure p is approximated in the following space:

$$M_k = Q_k \cap L_0^2(\Omega), \tag{3.5}$$

where $\mathbb{P}_m$ denotes the space of polynomials of degree m, and Q_k is the linear finite element space.

$$Q_k = \left\{ q \in C^0(\bar{\Omega}) : \forall T \in \mathcal{T}_k, q|_T \in \mathbb{P}_1 \right\}.$$

With these spaces, we can have the k-th level discrete formulation of the problem (3.1),(3.2):

$$\begin{aligned} \frac{\mu}{\rho}\int_\Omega \left(\boldsymbol{K}^{-1}\boldsymbol{u}_k\right)\cdot\boldsymbol{\varphi}_k\,d\boldsymbol{x} + \frac{\beta}{\rho}\int_\Omega |\boldsymbol{u}_k|\,(\boldsymbol{u}_k\cdot\boldsymbol{\varphi}_k)\,d\boldsymbol{x} \\ + \sum_{T\in\mathcal{T}_k}\int_T \nabla p_k\cdot\boldsymbol{\varphi}_k\,d\boldsymbol{x} = \int_\Omega \boldsymbol{f}\cdot\boldsymbol{\varphi}_k\,d\boldsymbol{x}, \quad \forall\boldsymbol{\varphi}_k \in X_k, \end{aligned} \tag{3.6}$$

$$\sum_{T\in\mathcal{T}_k}\int_T \nabla q_k\cdot\boldsymbol{u}_k\,d\boldsymbol{x} = -\int_\Omega g q_k\,d\boldsymbol{x} + \int_{\partial\Omega} g_N q_k\,d\boldsymbol{x}, \quad \forall q_k \in M_k. \tag{3.7}$$

In universal practice,

$$h_{k-1} = 2h_k, \quad \text{for } k = 2, 3, \dots.$$

Note that $\mathcal{T}_k$ are nested meshes, and thus

$$X_{k-1} \subset X_k, M_{k-1} \subset M_k.$$

In [18], the authors demonstrated that the discrete problem has a unique solution. Moreover, if $\mathcal{T}_k$ is shape regular with mesh size h and the solution $\boldsymbol{u}$ belongs to $W^{1,4}(\Omega)$ and p belongs to $W^{2,\frac{3}{2}}(\Omega)$, then the following error estimations are obtained in [18](Theorem 4.10):

$$\|\boldsymbol{u} - \boldsymbol{u}_h\|_{L^2(\Omega)} \le Ch|\boldsymbol{u}|_{W^{1,4}(\Omega)}, \tag{3.8}$$

$$\|\nabla(p - p_h)\|_{L^{\frac{3}{2}}(T)} \le Ch\left(|p|_{W^{2,\frac{3}{2}}(\Omega)} + \|u\|_{W^{1,4}(\Omega)}\right). \tag{3.9}$$

4. Nonlinear Iteration

In this section, we present the Peaceman-Rachford (PR) type method developed in [9] to decouple the nonlinearity and the constraint.

First, choose an initial guess $\left(\boldsymbol{u}_k^0, p_k^0\right)$ by solving a linear Darcy equation:

$$\frac{\mu}{\rho}\int_\Omega \left(\boldsymbol{K}^{-1}\boldsymbol{u}_k^0\right)\cdot\boldsymbol{\varphi}_k\,d\boldsymbol{x}+\sum_{T\in\mathcal{T}_k}\int_T \nabla p_k^0\cdot\boldsymbol{\varphi}_k\,d\boldsymbol{x}=\int_\Omega \boldsymbol{f}\cdot\boldsymbol{\varphi}_k\,d\boldsymbol{x},\ \forall\boldsymbol{\varphi}_k\in X_k, \tag{4.1}$$

$$\sum_{T\in\mathcal{T}_k}\int_T \nabla q_k\cdot\boldsymbol{u}_k^0\,d\boldsymbol{x}=-\int_\Omega g q_k\,d\boldsymbol{x}+\int_{\partial\Omega} g_N q_k\,d\boldsymbol{x},\ \forall q_k\in M_k. \tag{4.2}$$

The linear Darcy system (4.1) and (4.2) can be rewritten in the matrix form as

$$\begin{bmatrix} A & B\\ B^T & 0\end{bmatrix}\begin{bmatrix}\boldsymbol{u}\\ p\end{bmatrix}=\begin{bmatrix}\boldsymbol{f_d}\\ w\end{bmatrix}, \tag{4.3}$$

where A is the symmetric and positive definite matrix associated to the term

$$\frac{\mu}{\rho}\int_\Omega \left(\boldsymbol{K}^{-1}\boldsymbol{u}_k\right)\cdot\boldsymbol{\varphi}_k\,d\boldsymbol{x},$$

B is the matrix corresponding to

$$\sum_{T\in\mathcal{T}_k}\int_T \nabla p_k\cdot\boldsymbol{\varphi}_k\,d\boldsymbol{x},$$

and $\boldsymbol{f_d}$ and w represent the right hand side of (4.1) and (4.2), respectively.

Then, knowing $\left(\boldsymbol{u}_k^0, p_k^0\right)$, construct a sequence $\left(\boldsymbol{u}_k^{n+1}, p_k^{n+1}\right)$ for $n\geq 0$ in two steps: Let α be a positive parameter chosen to enhance the convergence.

1. A nonlinear step without constraint: knowing $(\boldsymbol{u}_k^n, p_k^n)$ compute the intermediate velocity $\boldsymbol{u}_k^{n+\frac{1}{2}}$ by solving the following equation:

$$\begin{aligned}&\frac{1}{\alpha}\int_\Omega\left(\boldsymbol{u}_k^{n+\frac{1}{2}}-\boldsymbol{u}_k^n\right)\cdot\boldsymbol{\varphi}_k d\boldsymbol{x}+\frac{\beta}{\rho}\int_\Omega\left|\boldsymbol{u}_k^{n+\frac{1}{2}}\right|\left(\boldsymbol{u}_k^{n+\frac{1}{2}}\cdot\boldsymbol{\varphi}_k\right)d\boldsymbol{x}=\int_\Omega\boldsymbol{f}\cdot\boldsymbol{\varphi}_k\,d\boldsymbol{x}\\ &-\frac{\mu}{\rho}\int_\Omega\left(\boldsymbol{K}^{-1}\boldsymbol{u}_k^n\right)\cdot\boldsymbol{\varphi}_k d\boldsymbol{x}-\sum_{T\in\mathcal{T}_k}\int_T\nabla p_k^n\cdot\boldsymbol{\varphi}_k\,d\boldsymbol{x},\quad\forall\boldsymbol{\varphi}_k\in X_k.\end{aligned} \tag{4.4}$$

2. A linear step with constraint: compute $\left(\boldsymbol{u}_k^{n+1}, p_k^{n+1}\right)$ with the known $\boldsymbol{u}_k^{n+\frac{1}{2}}$

$$\begin{aligned}&\frac{1}{\alpha}\int_\Omega\left(\boldsymbol{u}_k^{n+1}-\boldsymbol{u}_k^{n+\frac{1}{2}}\right)\cdot\boldsymbol{\varphi}_k d\boldsymbol{x}+\frac{\mu}{\rho}\int_\Omega\left(\boldsymbol{K}^{-1}\boldsymbol{u}_k^{n+1}\right)\cdot\boldsymbol{\varphi}_k d\boldsymbol{x}+\sum_{T\in\mathcal{T}_k}\int_T\nabla p_k^{n+1}\cdot\boldsymbol{\varphi}_k\,d\boldsymbol{x}\\ &=\int_\Omega\boldsymbol{f}\cdot\boldsymbol{\varphi}_k\,d\boldsymbol{x}-\frac{\beta}{\rho}\int_\Omega\left|\boldsymbol{u}_k^{n+\frac{1}{2}}\right|\left(\boldsymbol{u}_k^{n+\frac{1}{2}}\cdot\boldsymbol{\varphi}_k\right)d\boldsymbol{x},\quad\forall\boldsymbol{\varphi}_k\in X_k,\end{aligned} \tag{4.5}$$

$$\sum_{T\in\mathcal{T}_k}\int_T\nabla q_k\cdot\boldsymbol{u}_k^{n+1}\,d\boldsymbol{x}=-\int_\Omega g q_k\,d\boldsymbol{x}+\int_{\partial\Omega}g_N q_k\,d\boldsymbol{x},\quad\forall q_k\in M_k. \tag{4.6}$$

A key observation in [9] is that because the test functions $\boldsymbol{\varphi}_k$, the solution $\boldsymbol{u}_k^{n+\frac{1}{2}}$, and ∇p_k^n are constant in each element T, the nonlinear step (4.4) can be solved as follows:

$$\boldsymbol{u}_T^{n+\frac{1}{2}} = \frac{1}{\gamma}\boldsymbol{F}_T^{n+\frac{1}{2}} \tag{4.7}$$

where

$$\begin{aligned}
\boldsymbol{F}_T^{n+\frac{1}{2}} &= \frac{1}{\alpha}\boldsymbol{u}_T^n - \frac{\mu}{\rho}\boldsymbol{K}_T^{-1}\boldsymbol{u}_T^n - \nabla_T p_k^n + \boldsymbol{f}_T,\\
\boldsymbol{K}_T^{-1} &= \frac{1}{|T|}\int_T \boldsymbol{K}^{-1}(\boldsymbol{x})\,d\boldsymbol{x},\\
\gamma &= \frac{1}{2\alpha} + \frac{1}{2}\sqrt{\frac{1}{\alpha^2} + 4\frac{\beta}{\rho}\left|\boldsymbol{F}_T^{n+\frac{1}{2}}\right|}.
\end{aligned}$$

In the second step, the linear system (4.5) and (4.6) can be rewritten in the following matrix form:

$$\begin{bmatrix} A_\alpha & B \\ B^T & 0 \end{bmatrix}\begin{bmatrix} \boldsymbol{u} \\ p \end{bmatrix} = \begin{bmatrix} \boldsymbol{f}_{\boldsymbol{n+\frac{1}{2}}} \\ w \end{bmatrix}, \tag{4.8}$$

where A_α is the matrix corresponding to

$$\frac{1}{\alpha}\int_\Omega \left(\boldsymbol{u}_k^{n+1}\right)\cdot\boldsymbol{\varphi}_k d\boldsymbol{x} + \frac{\mu}{\rho}\int_\Omega \left(\boldsymbol{K}^{-1}\boldsymbol{u}_k^{n+1}\right)\cdot\boldsymbol{\varphi}_k d\boldsymbol{x},$$

and $\boldsymbol{f}_{\boldsymbol{n+\frac{1}{2}}}$ is the vector corresponding to

$$\int_\Omega \boldsymbol{f}\cdot\boldsymbol{\varphi}_k\,d\boldsymbol{x} + \frac{1}{\alpha}\int_\Omega \left(\boldsymbol{u}_k^{n+\frac{1}{2}}\right)\cdot\boldsymbol{\varphi}_k d\boldsymbol{x} - \frac{\beta}{\rho}\int_\Omega \left|\boldsymbol{u}_k^{n+\frac{1}{2}}\right|\left(\boldsymbol{u}_k^{n+\frac{1}{2}}\cdot\boldsymbol{\varphi}_k\right)d\boldsymbol{x}.$$

In [9], the authors proved that (4.1), (4.2) and (4.5), (4.6) have a unique solution. The iterative method is convergent for an arbitrary choice of the initial guess $\left(\boldsymbol{u}_k^0, p_k^0\right)$ and an arbitrary positive α. Numerically, choice of α will affect the convergence of the nonlinear iteration. We shall report a good choice of this parameter.

We can reduce the linear saddle point system into a SPD system. Because of A and A_α are symmetric positive definite operators, without loss of generality, we take (4.8) as an example to expound an idea as follows:

Eliminate $\boldsymbol{u}$ from the first equation of (4.8), i.e.

$$\boldsymbol{u} = A_\alpha^{-1}\left(\boldsymbol{f}_{\boldsymbol{n+\frac{1}{2}}} - Bp\right), \tag{4.9}$$

and then, substituting to the second equation of (4.8), we get

$$Mp = b, \tag{4.10}$$

where $M = B^T A_\alpha^{-1} B, b = B^T A_\alpha^{-1}\boldsymbol{f}_{\boldsymbol{n+\frac{1}{2}}} - w$. After solving (4.10), we can get $\boldsymbol{u}$ by solving (4.9).

Since A_α is block-diagonal, A_α^{-1} can be formed easily. Equation (4.10) is the linear finite element dscretization of an elliptic equation in primary formulation. Solving the SPD system (4.10) is much easier than the saddle point system (4.8) and many fast solvers are available. The equivalence between (4.9),(4.10) and (4.8) is obvious.

5. Multigrid Algorithm

In this section, we consider a generic system of nonlinear equations,

$$\mathcal{L}(\boldsymbol{z}) = \boldsymbol{s}$$

where $\boldsymbol{z}, \boldsymbol{s} \in \boldsymbol{R}^{\boldsymbol{n}}$. Suppose that $\boldsymbol{v}$ is an approximation to the exact solution $\boldsymbol{z}$. Define the error $\boldsymbol{e}$ and the residual $\boldsymbol{r}$:

$$\begin{aligned} \boldsymbol{e} &= \boldsymbol{z} - \boldsymbol{v}, \\ \boldsymbol{r} &= \boldsymbol{s} - \mathcal{L}(\boldsymbol{v}). \end{aligned}$$

We can solve this nonlinear system by using some iterative solver,

$$\mathcal{L}_k(\boldsymbol{z}) = \boldsymbol{s},$$

here k means the discrete problem on the k-th level mesh $\mathcal{T}_k$.

Because of the iterative nature, multigird ideas should be effective on the nonlinear problem. The multigrid scheme here we used for this nonlinear problem is the most commonly used nonlinear version of multigrid. It is called the *full approximation scheme* (FAS) [3] because the problem in the coarse grid is solved for the full approximation $\boldsymbol{z}_{k-1} = I_k^{k-1}\boldsymbol{v}_k + \boldsymbol{e}_{k-1}$ rather than the error $\boldsymbol{e}_{k-1}$. A V-cycle multigrid scheme is described as follows:

Full Approximation Scheme (FAS).

- Pre-smoothing: For $1 \leq j \leq m$, relax m times with an initial guess $\boldsymbol{v}_0$ by $\boldsymbol{v}_j = R_k \boldsymbol{v}_{j-1}$. The current approximation $\boldsymbol{v}_k = \boldsymbol{v}_m$.
- Restrict the current approximation and its fine grid residual to the coarse grid: $\boldsymbol{r}_{k-1} = I_k^{k-1}\left(\boldsymbol{s}_k - \mathcal{L}_k(\boldsymbol{v}_k)\right)$ and $\boldsymbol{v}_{k-1} = I_k^{k-1}\boldsymbol{v}_k$.
- Solve the coarse grid problem: $\mathcal{L}_{k-1}(\boldsymbol{z}_{k-1}) = \mathcal{L}_{k-1}(\boldsymbol{v}_{k-1}) + \boldsymbol{r}_{k-1}$.
- Compute the coarse grid approximation to the error: $\boldsymbol{e}_{k-1} = \boldsymbol{z}_{k-1} - \boldsymbol{v}_{k-1}$.
- Interpolate the error approximation up to the fine grid and correct the current fine grid approximation: $\boldsymbol{v}_{m+1} \leftarrow \boldsymbol{v}_k + I_{k-1}^k \boldsymbol{e}_{k-1}$.
- Post-smoothing: For $m+2 \leq j \leq 2m+1$, relax m times by $\boldsymbol{v}_j = R_k{}' \boldsymbol{v}_{j-1}$.

then we get the approximate solution $\boldsymbol{v}_{2m+1}$. Here m denotes the number of pre-smoothing and post-smoothing steps, R_k denotes the chosen relaxation method, and I_k^{k-1} is an intergrid transfer operator from the fine grid to the coarse grid.

We apply the PR iteration as the smoother R_k. We need to switch the ordering of the linear and nonlinear steps in the post-smoothing step in order to keep the symmetry of the V-cycle. It is worth pointing out that although the chosen finite element spaces are nested, the constrained subspaces are non-nested when we interpolated the correction of the velocity, which was obtained in the coarser space, to the finer space. Namely, if we directly interpolated the correction obtained on the coarser grid to the finer grid, the approximation we got do not satisfy the divergence equation in this Darcy-Forchheimer model. We need to construct a L^2 projection to map the correction

obtained before into the constrained space in the fine grid. This can be realized by solving a saddle point system:

$$\begin{bmatrix} A_{\boldsymbol{\delta}} & B \\ B^T & 0 \end{bmatrix} \begin{bmatrix} \boldsymbol{\delta} \\ \theta \end{bmatrix} = \begin{bmatrix} \mathbf{0} \\ B^T \boldsymbol{e_u} \end{bmatrix}, \tag{5.1}$$

where $A_{\boldsymbol{\delta}}$ is the matrix corresponding to

$$\frac{\mu}{\rho} \int_\Omega \left(\boldsymbol{K}^{-1}\boldsymbol{\delta}\right) \cdot \boldsymbol{\varphi}_k \, d\boldsymbol{x} + \frac{\beta}{\rho} \int_\Omega |\boldsymbol{v}| \left(\boldsymbol{\delta} \cdot \boldsymbol{\varphi}_k\right) d\boldsymbol{x},$$

$\boldsymbol{\delta}, \theta$ represent the error between the restriction of the approximation of velocity and pressure on the finer grid and their approximation obtained on the coarser grid, respectively, and $\boldsymbol{e_u}$ is the prolonged correction to the fine space.

Again, (5.1) can be reduced to a SPD system. We can get $\boldsymbol{\delta} = A_{\boldsymbol{\delta}}^{-1} B\theta$ through the idea demonstrated in Section 4. Then we obtain a corrected approximation of velocity $\boldsymbol{v} = \boldsymbol{v} - \boldsymbol{\delta}$, which satisfied the divergence equation.

6. Numerical Experiments

In this section, we present some numerical results to illustrate the efficiency of our multigrid method for the Darcy-Forchheimer equation (2.1)-(2.3). The following test problems were taken from [10]. All of our experiments are implemented based on the MATLAB© software package *i*FEM [4].

We choose $\mu = 1$, $\rho = 1$, $\boldsymbol{K} = \boldsymbol{I}$. $\Omega \subset \mathbb{R}^2$ is a square,

$$\Omega = \left\{(x, y) \in \mathbb{R}^2 : \ -1 < x < 1, \ -1 < y < 1\right\}.$$

Problem 1:

$$\begin{aligned} \boldsymbol{u}(x, y) &= [x + y, x - y]^T, \\ p(x, y) &= x^3 + y^3, \end{aligned}$$

$$\boldsymbol{f}(x, y) = \begin{bmatrix} \left(1 + \beta\sqrt{2x^2 + 2y^2}\right)(x + y) + 3x^2 \\ \left(1 + \beta\sqrt{2x^2 + 2y^2}\right)(x - y) + 3y^2 \end{bmatrix},$$

$$g_N(x, y) = \begin{cases} 1 + y, & x = 1, \\ 1 - y, & x = -1, \\ x - 1, & y = 1, \\ -x - 1, & y = -1. \end{cases}$$

Problem 2:

$$\begin{aligned} \boldsymbol{u}(x, y) &= \left[\frac{(x+1)^2}{4}, -\frac{(x+1)(y+1)}{2}\right]^T, \\ p(x, y) &= x^3 + y^3, \end{aligned}$$

$$\boldsymbol{f}(x,y)=\begin{bmatrix}\frac{(x+1)^2}{4}\left(1+\beta\frac{(x+1)}{4}\sqrt{(x+1)^2+4(y+1)^2}\right)+3x^2\\ -\frac{(x+1)(y+1)}{2}\left(1+\beta\frac{(x+1)}{4}\sqrt{(x+1)^2+4(y+1)^2}\right)+3y^2\end{bmatrix},$$

$$g_N(x,y)=\begin{cases}1, & x=1,\\ 0, & x=-1,\\ -x-1, & y=1,\\ 0, & y=-1.\end{cases}$$

For all above test problems, $g=0$. The chosen termination criterion is

$$r=r_u+r_p\leq tol,$$

where

$$r_u = \begin{cases}\left\|\boldsymbol{f}-\frac{\mu}{\rho}\boldsymbol{K}^{-1}\boldsymbol{u}_h^n+\frac{\beta}{\rho}\left|\boldsymbol{u}_h^n\right|\boldsymbol{u}_h^n+\nabla p_h^n\right\|/\left\|\boldsymbol{f}\right\|, & \text{when } \|\boldsymbol{f}\|\neq 0,\\ \left\|\boldsymbol{f}-\frac{\mu}{\rho}\boldsymbol{K}^{-1}\boldsymbol{u}_h^n+\frac{\beta}{\rho}\left|\boldsymbol{u}_h^n\right|\boldsymbol{u}_h^n+\nabla p_h^n\right\|, & \text{when } \|\boldsymbol{f}\|=0.\end{cases}$$

$$r_p = \begin{cases}\left\|g-\mathrm{div}\boldsymbol{u}_h^n\right\|/\left\|g\right\|, & \text{when } \|g\|\neq 0,\\ \left\|g-\mathrm{div}\boldsymbol{u}_h^n\right\|, & \text{when } \|g\|=0.\end{cases}$$

In the first test, we study that whether the accuracy will change according to different choices of tol. Numerical tests were performed for all these problems, and the behaviour of these experiments was similar for all these problems. Therefore, here we only posed the results when $\alpha=1,\beta=10$.

The letter N stands for 'Number of unknowns of p', which is the same as 'Numbers of vertices', so $h=\frac{2}{\sqrt{N}-1}$, which represents the discretization mesh size in one direction. The results confirmed the convergence order for $\|\boldsymbol{u}-\boldsymbol{u}_h\|_{L^2}$ and $\|p-p_h\|_{H^1}$ are $O(h)$. However, the accuracy of the pressure approximations in L^2-norm depends on tol. From Figure 1, it is clear that the L^2-norm of the pressure approximations when $tol=10^{-6}$ is better than the one when $tol=10^{-5}$ for Problem 1 and Problem 2. Meanwhile, in consideration of the computation cost, the sufficiently accurate results were achieved when $tol=10^{-6}$ for Problem 1 and 2. Therefore, the value of $tol=10^{-6}$ is used in the remaining numerical experiments. Instead, in [10] the authors use $tol=1.95h$, which only considered the L^2-norm approximation for velocity.

In the second test, we give an empirical choice of parameter $\alpha=1/\beta$. As it is mentioned in [9], the PR nonlinear iteration converges for any $\alpha>0$. Its convergence rate, however, is very sensitive to the choice of this parameter. From the convergence proof of the PR algorithm in [9], we inferred that the choices of α depends on β. Here we tested $\alpha=1/\beta$, then compared with the choice $\alpha=1$ in two aspects: the number of iterations (abbreviated as iter) and CPU time. As shown in Table 1 and 2, this choice of the parameter α is much better than the fixed selection for different values of β. Therefore, this choice of α will be used in the remaining numerical experiments.

In the following experiments, we compare the multigrid method with the PR iterative method for solving this nonlinear systems. Here we choose $m=3$ for all the following tests. It means that we apply three PR iterations in the pre-smoothing step and post-smoothing step, respectively. In order to keep the symmetry of the V-cycle, we switch the ordering of the linear and nonlinear steps in the post-smoothing step. We set $h=1/16$ as the initial mesh. In the tables, we use the following symbols: $E_{\boldsymbol{u},0}=\|\boldsymbol{u}-\boldsymbol{u}_h\|_{L^2}, E_{p,0}=\|p-p_h\|_{L^2}, E_{p,1}=\|p-p_h\|_{H^1}$.

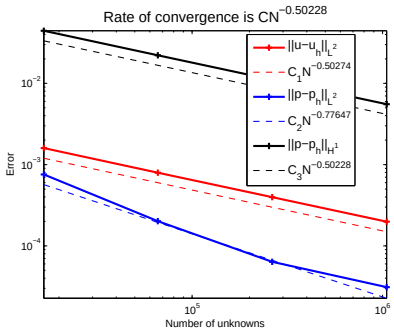

(a) Convergence Rate of Problem 1 with $tol = 10^{-5}$

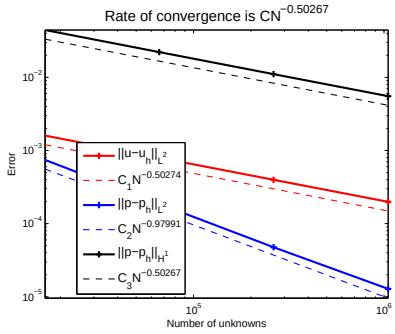

(b) Convergence Rate of Problem 1 with $tol = 10^{-6}$

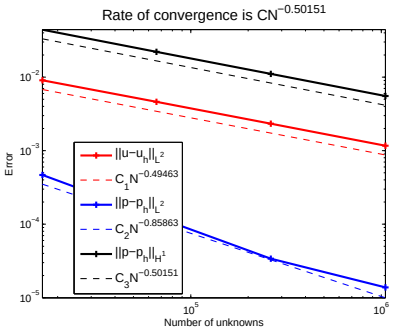

(c) Convergence Rate of Problem 2 with $tol = 10^{-5}$

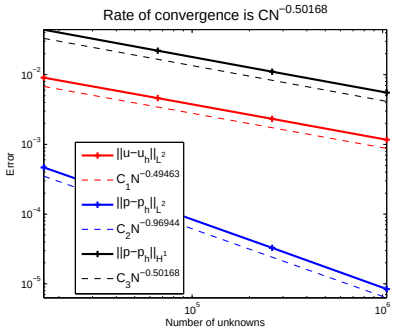

(d) Convergence Rate of Problem 2 with $tol = 10^{-6}$

FIGURE 1. Comparison of the convergence rate for Problem 1 and 2 with different *tols*.

TABLE 1. Comparison of different values of α with $h = \frac{1}{64}$ for $\beta = 10, 20, 30$.

Problem		$\beta = 10$		$\beta = 20$		$\beta = 30$	
		$\alpha = 1$	$\alpha = 1/10$	$\alpha = 1$	$\alpha = 1/20$	$\alpha = 1$	$\alpha = 1/30$
Problem 1	iter	229	73	457	105	686	120
	CPU time	14 s	4 s	26 s	6 s	38 s	7 s
Problem 2	iter	230	171	459	183	688	191
	CPU time	13 s	10 s	26 s	11 s	38 s	11 s

The PR solver is denoted by s, whereas the multigrid solver is denoted by m. I - number of iterations, and CPU - CPU time. 's1' represents that we solve those linear saddle point systems directly in each step while we use the PR iterative method to solve this nonlinear system, 's2' is that we solve the SPD system mentioned in Section 4 rather than solving the saddle point system directly. Our multigrid solver is constructed based on 's2'. In all examples we achieve optimal

TABLE 2. Comparison of different values of α with $h = \frac{1}{64}$ for $\beta = 40, 50, 60$.

Problem		$\beta = 40$		$\beta = 50$		$\beta = 60$	
		$\alpha = 1$	$\alpha = 1/40$	$\alpha = 1$	$\alpha = 1/50$	$\alpha = 1$	$\alpha = 1/60$
Problem 1	iter	914	126	1143	129	1371	131
	CPU time	53 s	7 s	66 s	7 s	79 s	8 s
Problem 2	iter	917	198	1146	205	1376	213
	CPU time	52 s	11 s	65 s	11 s	79 s	12 s

TABLE 3. Comparison of error of Problem 1 by using different solvers with $\beta = 10, \alpha = 1/10$.

h	dof	$E^{\mathrm{s}}_{\boldsymbol{u},0}$	$E^{\mathrm{s}}_{p,0}$	$E^{\mathrm{s}}_{p,1}$	$E^{\mathrm{m}}_{\boldsymbol{u},0}$	$E^{\mathrm{m}}_{p,0}$	$E^{\mathrm{m}}_{p,1}$
$\frac{1}{16}$	5,185	6.726e-3	1.181e-2	1.860e-1	6.726e-3	1.181e-2	1.860e-1
$\frac{1}{32}$	20,609	3.232e-3	2.960e-3	8.979e-2	3.232e-3	2.960e-3	8.979e-2
$\frac{1}{64}$	83,177	1.596e-3	7.404e-4	4.440e-2	1.596e-3	7.404e-4	4.440e-2
$\frac{1}{128}$	328,193	7.952e-4	1.851e-4	2.213e-2	7.953e-4	1.851e-4	2.213e-2
$\frac{1}{256}$	1,311,745	3.972e-4	4.628e-5	1.105e-2	3.973e-4	4.628e-5	1.105e-2
$\frac{1}{512}$	5,244,929	1.986e-4	1.157e-5	5.525e-3	1.986e-4	1.157e-5	5.525e-3
Rate	-	1.022	2.015	1.021	1.022	2.015	1.021

TABLE 4. Comparison of number of iterations and CPU time of Problem 1 by using different solvers with $\beta = 10$.

h	dof	I(s)	I(m)	CPU(s1)	CPU(s2)	CPU(m)
$\frac{1}{16}$	5,185	42	1	0.61 s	0.34 s	0.27 s
$\frac{1}{32}$	20,609	59	4	2.2 s	0.88 s	0.49 s
$\frac{1}{64}$	83,177	73	4	15.0 s	4.3 s	1.6 s
$\frac{1}{128}$	328,193	84	4	134.9 s	26.1 s	7.4 s
$\frac{1}{256}$	1,311,745	95	4	951.2 s	165.1 s	31.8 s
$\frac{1}{512}$	5,244,929	99	3	6827.7 s	875.4 s	160.5 s

order convergence of $\|\boldsymbol{u} - \boldsymbol{u}_h\|_{L^2}$ and $\|p - p_h\|_{H^1}$. Since our focus is on the efficiency of solvers, we mainly report the comparison of the number of iterations and CPU time by using different solvers.

It can be observed that our multigrid solver required significantly fewer iterations and CPU time than the other two solvers, and the time complexity of our multigrid solver is almost $O(N)$, in contrast, the time complexity of the other two solvers seems to be more computationally expensive than that of our solver, which demonstrated the efficiency of our approach. As shown in Table 9 and 16, the number of iterations are compared for different beta and it is demonstrated that our multigrid method is robust to both h and β.

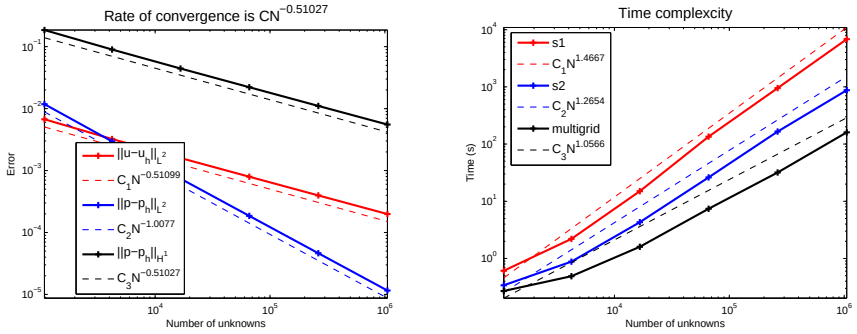

(a) Convergence rate by using multigrid solver (b) Time complexity

FIGURE 2. Convergence rate by using multigrid solver and time complexity by using different solvers for Problem 1 with $\beta = 10$.

TABLE 5. Comparison of number of iterations and CPU time of Problem 1 by using different solvers with $\beta = 20$.

h	dof	I(s)	I(m)	CPU(s1)	CPU(s2)	CPU(m)
$\frac{1}{16}$	5,185	49	1	0.68 s	0.43 s	0.34 s
$\frac{1}{32}$	20,609	75	6	2.7 s	1.1 s	0.62 s
$\frac{1}{64}$	83,177	105	6	24.6 s	5.1 s	2.0 s
$\frac{1}{128}$	328,193	126	5	195.1 s	32.5 s	9.5 s
$\frac{1}{256}$	1,311,745	139	5	1312.2 s	209.5 s	52.0 s
$\frac{1}{512}$	5,244,929	153	5	10354.2 s	1380.2 s	219.2 s

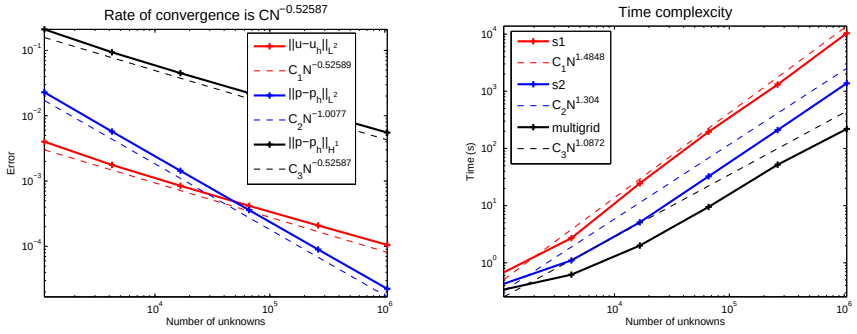

(a) Convergence rate by using multigrid solver (b) Time complexity

FIGURE 3. Convergence rate by using multigrid solver and time complexity by using different solvers for Problem 1 with $\beta = 20$.

TABLE 6. Comparison of number of iterations and CPU time of Problem 1 by using different solvers with $\beta = 30$.

h	dof	I(s)	I(m)	CPU(s1)	CPU(s2)	CPU(m)
$\frac{1}{16}$	5,185	50	1	0.70 s	0.43 s	0.34 s
$\frac{1}{32}$	20,609	81	6	3.0 s	1.1 s	0.65 s
$\frac{1}{64}$	83,177	120	6	28.6 s	6.6 s	2.3 s
$\frac{1}{128}$	328,193	154	6	242.3 s	48.8 s	12.1 s
$\frac{1}{256}$	1,311,745	168	6	1554.7 s	308.3 s	56.5 s
$\frac{1}{512}$	5,244,929	185	5	11857.3 s	1667.7 s	254.6 s

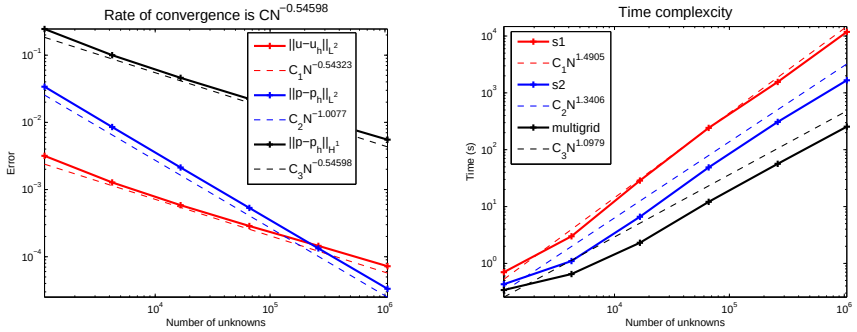

(a) Convergence rate by using multigrid solver (b) Time complexity

FIGURE 4. Convergence rate by using multigrid solver and time complexity by using different solvers for Problem 1 with $\beta = 30$.

TABLE 7. Comparison of number of iterations and CPU time of Problem 1 by using different solvers with $\beta = 40$.

h	dof	I(s)	I(m)	CPU(s1)	CPU(s2)	CPU(m)
$\frac{1}{16}$	5,185	50	1	0.80 s	0.43 s	0.35 s
$\frac{1}{32}$	20,609	82	7	3.1 s	1.1 s	0.70 s
$\frac{1}{64}$	83,177	126	7	30.5 s	7.7 s	2.4 s
$\frac{1}{128}$	328,193	171	6	269.9 s	59.5 s	13.1 s
$\frac{1}{256}$	1,311,745	192	6	1786.3 s	329.6 s	63.9 s
$\frac{1}{512}$	5,244,929	207	6	13504.1 s	1819.4 s	270.4 s

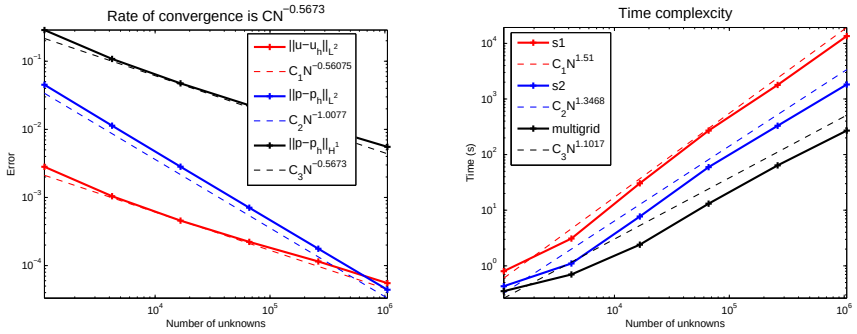

(a) Convergence rate by using multigrid solver (b) Time complexity

FIGURE 5. Convergence rate by using multigrid solver and time complexity by using different solvers for Problem 1 with $\beta = 40$.

TABLE 8. Comparison of number of iterations and CPU time of Problem 1 by using different solvers with $\beta = 50$.

h	dof	I(s)	I(m)	CPU(s1)	CPU(s2)	CPU(m)
$\frac{1}{16}$	5,185	50	1	0.91 s	0.45 s	0.35 s
$\frac{1}{32}$	20,609	82	7	3.1 s	1.1 s	0.72 s
$\frac{1}{64}$	83,177	129	7	31.4 s	7.9 s	2.6 s
$\frac{1}{128}$	328,193	181	7	312.6 s	61.9 s	13.5 s
$\frac{1}{256}$	1,311,745	210	6	1955.6 s	371.1 s	64.8 s
$\frac{1}{512}$	5,244,929	222	6	14733.5 s	2009.4 s	306.8 s

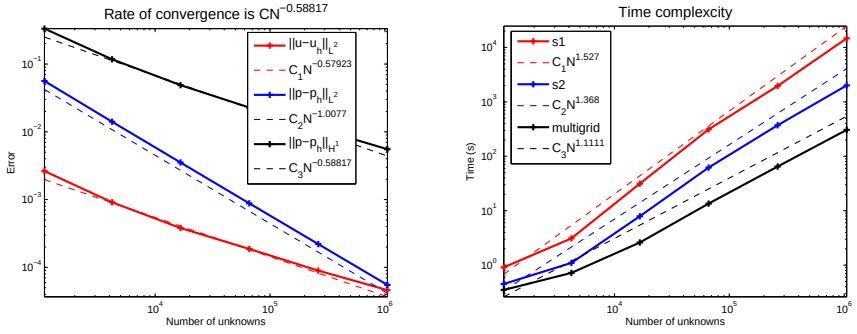

(a) Convergence rate by using multigrid solver (b) Time complexity

FIGURE 6. Convergence rate by using multigrid solver and time complexity by using different solvers for Problem 1 with $\beta = 50$.

TABLE 9. Comparison of iteration steps of multigrid solver according to different h and β for Problem 1 with $\alpha = 1/\beta$.

h	$\beta = 10$	$\beta = 20$	$\beta = 30$	$\beta = 40$	$\beta = 50$
$\frac{1}{32}$	4	6	6	7	7
$\frac{1}{64}$	4	6	6	7	7
$\frac{1}{128}$	4	5	6	6	7
$\frac{1}{256}$	4	5	6	6	6
$\frac{1}{512}$	3	5	5	6	6

TABLE 10. Comparison of error of Problem 2 by using different solvers with $\beta = 10, \alpha = 1/10$.

h	dof	$E^{\mathrm{s}}_{\boldsymbol{u},0}$	$E^{\mathrm{s}}_{p,0}$	$E^{\mathrm{s}}_{p,1}$	$E^{\mathrm{m}}_{\boldsymbol{u},0}$	$E^{\mathrm{m}}_{p,0}$	$E^{\mathrm{m}}_{p,1}$
$\frac{1}{16}$	5,185	3.244e-2	5.863e-3	1.772e-1	3.244e-2	5.863e-3	1.772e-1
$\frac{1}{32}$	20,609	1.740e-2	1.680e-3	8.846e-2	1.740e-2	1.680e-3	8.846e-2
$\frac{1}{64}$	83,177	9.048e-3	4.676e-4	4.421e-2	9.042e-3	4.676e-4	4.421e-2
$\frac{1}{128}$	328,193	4.610e-3	1.258e-4	2.210e-2	4.601e-3	1.250e-4	2.210e-2
$\frac{1}{256}$	1,311,745	2.323e-3	3.285e-5	1.105e-2	2.314e-3	3.250e-5	1.105e-2
$\frac{1}{512}$	5,244,929	1.165e-3	8.448e-6	5.524e-3	1.159e-3	8.288e-6	5.524e-3
Rate	-	0.970	1.904	1.009	0.972	1.910	1.009

TABLE 11. Comparison of number of iterations and CPU time of Problem 2 by using different solvers with $\beta = 10$.

h	dof	I(s)	I(m)	CPU(s1)	CPU(s2)	CPU(m)
$\frac{1}{16}$	5,185	75	1	0.87 s	0.51 s	0.29 s
$\frac{1}{32}$	20,609	111	5	4.0 s	1.4 s	0.95 s
$\frac{1}{64}$	83,177	171	5	42.6 s	10.7 s	2.4 s
$\frac{1}{128}$	328,193	269	5	437.3 s	91.8 s	8.7 s
$\frac{1}{256}$	1,311,745	428	4	3983.2 s	733.5 s	43.2 s
$\frac{1}{512}$	5,244,929	686	4	$>$ 13 hours	6331.6 s	203.3 s

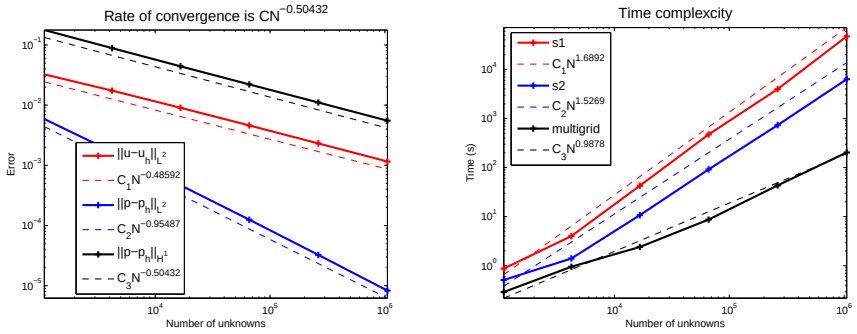

(a) Convergence rate by using multigrid solver (b) Time complexity

FIGURE 7. Convergence rate by using multigrid solver and time complexity by using different solvers for Problem 2 with $\beta = 10$.

TABLE 12. Comparison of number of iterations and CPU time of Problem 2 by using different solvers with $\beta = 20$.

h	dof	I(s)	I(m)	CPU(s1)	CPU(s2)	CPU(m)
$\frac{1}{16}$	5,185	84	1	0.94 s	0.52 s	0.36 s
$\frac{1}{32}$	20,609	121	7	4.1 s	1.5 s	0.96 s
$\frac{1}{64}$	83,177	183	7	45.8 s	11.3 s	3.0 s
$\frac{1}{128}$	328,193	288	7	465.8 s	93.8 s	15.3 s
$\frac{1}{256}$	1,311,745	459	6	4338.6 s	776.5 s	65.5 s
$\frac{1}{512}$	5,244,929	732	5	$>$ 13 hours	6350.6 s	268.4 s

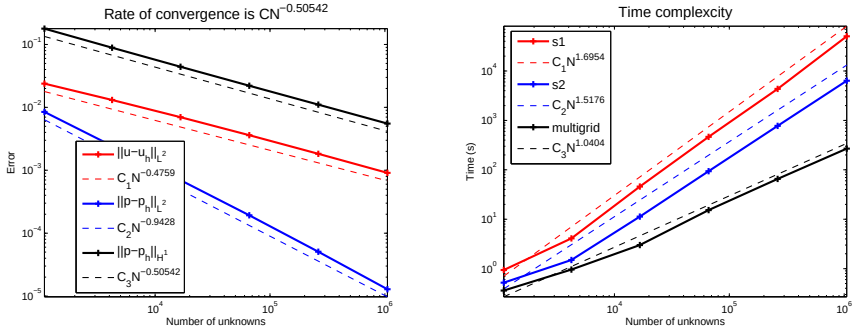

(a) Convergence rate by using multigrid solver (b) Time complexity

FIGURE 8. Convergence rate by using multigrid solver and time complexity by using different solvers for Problem 2 with $\beta = 20$.

TABLE 13. Comparison of number of iterations and CPU time of Problem 2 by using different solvers with $\beta = 30$.

h	dof	I(s)	I(m)	CPU(s1)	CPU(s2)	CPU(m)
$\frac{1}{16}$	5,185	92	1	0.96 s	0.54 s	0.39 s
$\frac{1}{32}$	20,609	128	9	4.6 s	1.6 s	1.0 s
$\frac{1}{64}$	83,177	191	9	46.5 s	11.8 s	3.8 s
$\frac{1}{128}$	328,193	296	9	462.9 s	98.3 s	18.2 s
$\frac{1}{256}$	1,311,745	468	8	4412.9 s	792.6 s	83.6 s
$\frac{1}{512}$	5,244,929	746	7	$>$ 14 hours	6440.3 s	357.2 s

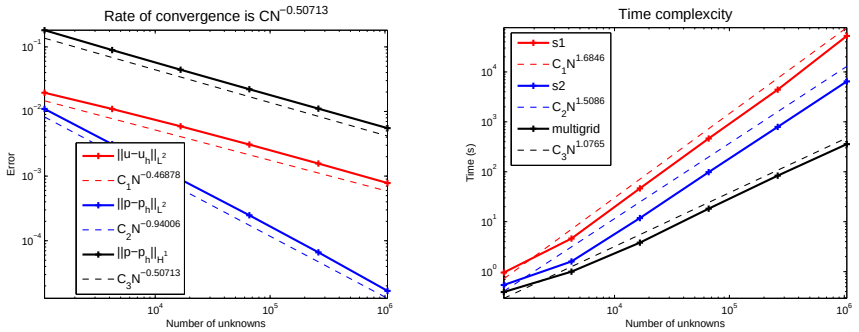

(a) Convergence rate by using multigrid solver (b) Time complexity

FIGURE 9. Convergence rate by using multigrid solver and time complexity by using different solvers for Problem 2 with $\beta = 30$.

TABLE 14. Comparison of number of iterations and CPU time of Problem 2 by using different solvers with $\beta = 40$.

h	dof	I(s)	I(m)	CPU(s1)	CPU(s2)	CPU(m)
$\frac{1}{16}$	5,185	100	1	1.0 s	0.63 s	0.39 s
$\frac{1}{32}$	20,609	134	11	4.6 s	1.6 s	1.1 s
$\frac{1}{64}$	83,177	198	11	49.9 s	12.1 s	4.2 s
$\frac{1}{128}$	328,193	306	10	500.4 s	98.8 s	21.6 s
$\frac{1}{256}$	1,311,745	481	9	4532.5 s	802.5 s	96.1 s
$\frac{1}{512}$	5,244,929	759	8	$>$ 15 hours	6875.1 s	405.1 s

7. CONCLUSIONS

In this paper, we constructed a nonlinear multigrid method for a mixed finite element method of the two-dimensional Darcy-Forchheimer model. We presented a comparative study between the multigrid solver and the PR iterative solver, at the same time compared CPU time of the efficient solver of solving the SPD systems with that obtained by solving the linear saddle point systems

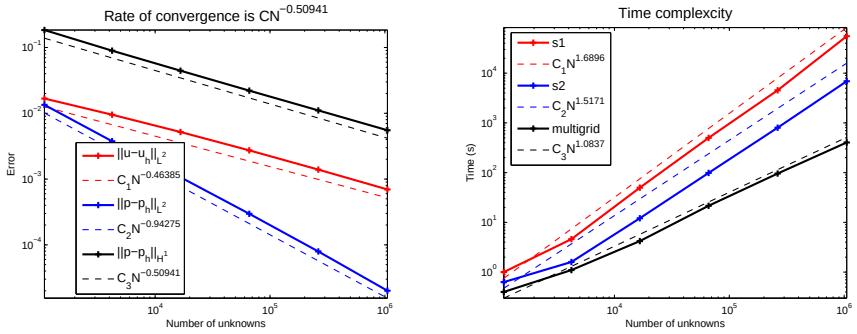

(a) Convergence rate by using multigrid solver (b) Time complexity

FIGURE 10. Convergence rate by using multigrid solver and time complexity by using different solvers for Problem 2 with $\beta = 40$.

TABLE 15. Comparison of number of iterations and CPU time of Problem 2 by using different solvers with $\beta = 50$.

h	dof	I(s)	I(m)	CPU(s1)	CPU(s2)	CPU(m)
$\frac{1}{16}$	5,185	109	1	1.1 s	0.62 s	0.42 s
$\frac{1}{32}$	20,609	142	12	4.8 s	1.8 s	1.2 s
$\frac{1}{64}$	83,177	205	12	52.7 s	12.8 s	5.2 s
$\frac{1}{128}$	328,193	313	11	513.3 s	108.7 s	24.4 s
$\frac{1}{256}$	1,311,745	489	10	4729.3 s	850.1 s	108.5 s
$\frac{1}{512}$	5,244,929	770	9	$>$ 15 hours	6900.3 s	458.6 s

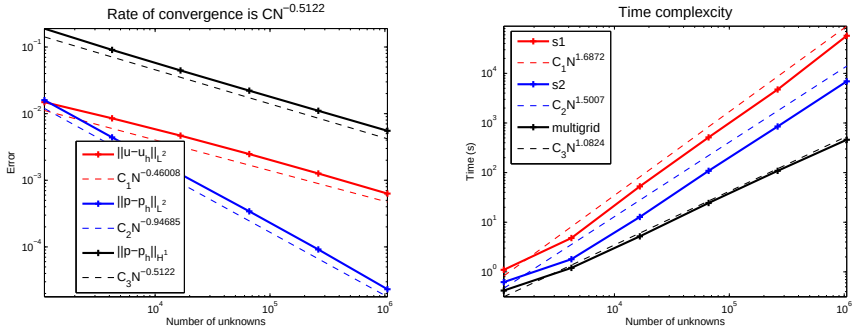

(a) Convergence rate by using multigrid solver (b) Time complexity

FIGURE 11. Convergence rate by using multigrid solver and time complexity by using different solvers for Problem 2 with $\beta = 50$.

TABLE 16. Comparison of iteration steps of multigrid solver according to different h and β for Problem 2 with $\alpha = 1/\beta$.

h	$\beta = 10$	$\beta = 20$	$\beta = 30$	$\beta = 40$	$\beta = 50$
$\frac{1}{32}$	5	7	9	11	12
$\frac{1}{64}$	5	7	9	11	12
$\frac{1}{128}$	5	7	9	10	11
$\frac{1}{256}$	4	6	8	9	10
$\frac{1}{512}$	4	5	7	8	9

directly. We took into account the pressure accuracy when we set the termination criterion, and chose a better value of the stopping criterion *tol*. In comparison with the authors in [10] always chose $\alpha = 1$ for different values of β, we reported a better choice and compared with the previous choice through comparing the number of iterations and CPU time. The results obtained from our tests indicate that the multigrid solver is very efficient for numerically solving this nonlinear elliptic equation. The number of iterations and CPU time for using multigrid solver are shown to be significantly less than that obtained by using the other solvers.

In the future work, we shall extend our results to two directions. One is that we would like to find a better smoother, which is used in the pre-smoothing and post-smoothing step, to reduce CPU time and make the multigrid solver more efficient. Another is that we intend to carry out some studies on the three-dimensional Darcy-Forchheimer problem and the real application in a porous medium.

REFERENCES

[1] Adams, R. A., Sobolev Spaces, Academic Press, New York (1975)

[2] Aziz, K., Settari, A., Petroleum Reservoir Simulation, Applied Science Publishers LTD, London (1979)

[3] Briggs, W. L., Henson, V. E., McCormick, S. F., A Multigrid tutorial, 2ndEdition, SIAM, Philadelphia (2000)

[4] Chen, L., *i*FEM: an integrated finite element methods package in MATLAB, Technical Report, Technical Report, University of California at Irvine (2009)

[5] Chen, L., Multigrid methods for saddle point systems using constrained smoothers, Computers and Mathematics with Applications, 70(12), 2854-2866 (2015)

[6] Ciarlet, P. G., The Finite Element Method for Elliptic Problems, North-Holland, Amsterdam, New York, Oxford (1978)

[7] Crouzeix, M., Raviart, P. A., Conforming and nonconforming finite element methods for solving the stationary Stokes equations I, RAIRO Anal. Numér, 7(3), 33-75 (1973)

[8] Forchheimer, P., Wasserbewegung durch Boden, Z. Ver. Deutsch. Ing., 45, 1782-1788 (1901)

[9] Girault, V., Wheeler, M. F., Numerical discretization of a Darcy-Forchheimer model, Numer. Math., 110(2), 161-198 (2008)

[10] López, H., Molina, B., Salas, José J., Comparison between different numerical discretizations for a DarcyForchheimer model, ETNA 34, 187-203 (2009)

[11] Pan, H., Rui, H., Mixed element method for two-dimensional Darcy-Forchheimer model, J.Sci. Comput., 52(3), 563-587 (2012)

[12] Park, E. J., Mixed finite element method for generalized Forchheimer flow in porous media, Numer. Methods Partial Differential Equations, 21(2), 213-228 (2005)

[13] Peaceman, D. W., Rachford, H. H., The numerical solution of parabolic and elliptic differential equations, J. Soc. Indust. Appl. Math., 3(2), 28-41 (1955)

[14] Rui, H., Liu, W., A two-grid block-centered finite difference method for Darcy-Forchheimer flow in porous media, SIAM J. Numer. Anal., 53(4), 1941-1962 (2015)

[15] Rui, H., Pan, H., A block-centered finite difference method for the Darcy-Forchheimer model, SIAM J. Numer. Anal., 50(5), 2612-2631 (2012)
[16] Rui, H., Zhao, D., Pan H., A block-centered finite difference method for Darcy-Forchheimer model with variable Forchheimer number, Numer. Methods Partial Differential Equations,31(5), 1603-1622 (2015)
[17] Ruth, D., Ma, H., On the derivation of the Forchheimer equation by means of the averaging theorem, Transport in Porous Media, 7(3), 255-264 (1992)
[18] Salas, José J., López, H., Molina, B., An analysis of a mixed finite element method for a DarcyForchheimer model, Mathematical and Computer Modelling, 57(9), 2325-2338 (2013)
[19] Wang, Y., Rui, H., Stabilized CrouzeixRaviart element for DarcyForchheimer model, Numer. Methods Partial Differential Equations, 31(5), 1568-1588.(2015)

(Jian Huang) School of Mathematics, Shandong University, Jinan, Shandong, CHINA 250100

(Long Chen) Department of Mathematics, University of California at Irvine, Irvine, CA, U.S.A 92697

(Hongxing Rui) School of Mathematics, Shandong University, Jinan, Shandong, CHINA 250100
E-mail address, Jian Huang: yghuangjian@sina.com
E-mail address, Long Chen: chenlong@math.uci.edu
E-mail address, Hongxing Rui: hxrui@sdu.edu.cn